Anal. Chem. **1998,** *70,* 2576−2583

Time-Resolved Fluorescence Monitoring of Aromatic Radicals in Photoinitiated Processes

Stephanie R. Shield and Joel M. Harris*

Department of Chemistry, University of Utah, Salt Lake City, Utah 84112

Photolytic initiation of free radical reactions is important to many areas of technology; time-resolved monitoring of submicromolar concentrations of radicals produced during the course of these reactions is needed to provide information about the rate of initiation and its competition with radical recombination. In this work, time-resolved laser-induced fluorescence is evaluated for monitoring of diphenylketyl radicals produced by photoreduction of the triplet state of benzophenone. Fluorescence from the doublet−doublet transition of the radical is excited with a continuous wave laser and provides a sensitive method to detect these intermediates at nanomolar concentrations and to study their kinetics in solution on time scales from a few microseconds to hundreds of milliseconds. The ketyl radical fluorescence measurements of radical initiation reactions allowed the H atom abstraction rate constant by triplet benzophenone from both 2-propanol and benzhydrol to be determined, where $k_H = (2.1 \pm 0.1) \times 10^6$ M^{-1} s^{-1} for 2-propanol and $k_H = (4.4 \pm 0.1) \times 10^6$ M^{-1} s^{-1} for benzhydrol. The diphenylketyl radical recombination rate constant was also determined by time-resolved fluorescence monitoring of the decay of the radical population and found to be $k_r = (1.9 \pm 0.2) \times 10^8$ M^{-1} s^{-1}. Formation kinetics could be measured on a microsecond time scale from radical populations as low as 45 nM; decay kinetics could be followed on a millisecond time scale from 20 nM radical concentrations.

Time-resolved monitoring of the kinetics of photoinitiated free radical reactions is an important but challenging analytical problem. The photolytic generation of free radicals is important to many areas of technology, including the synthesis of organic compounds, the synthesis and modification of polymer materials, and the photobinding of molecules to surfaces. In these applications, the performance of the materials depends sensitively on their reactivity, where the rates of reactions dictate the product yield, molecular weight, or degree of curing or cross-linking.

Aromatic ketones, including benzophenones, xanthones, and quinones, are commonly used as type II photoinitiators for ultraviolet curing of polymer resins, including thin films and coatings.[1,2] The low-lying n,π^* triplet state of these ketones, produced from ground-state absorption of UV radiation, acts as a precursor to curing and undergoes a hydrogen atom abstraction from an H atom donor to produce a diphenylketyl radical from the excited ketone and an alkyl radical from the H atom donor. Monitoring the kinetics of radical intermediates during their formation and subsequent decay can provide important information on the initiation of photocuring and its competition with radical recombination.

Despite the importance of measuring the rates of photoinitiation of free radical reactions, few analytical techniques are capable of direct time-resolved monitoring of the progress of these reactions, due to the combined need for speed and sensitivity. Monitoring the transient absorption of ketyl radical intermediates has been done to detect their formation from triplet states of aromatic ketones.[3−20] Flash photolysis is a useful approach for detecting higher concentrations (>10 μM) of transient species in photochemical processes. In applications of triplet precursors to photoinitiated free radical chain reactions, however, concentrations of the initiator must be kept low to avoid competition by radical recombination reactions, which reduce the yield of chain propagation reactions and lower the efficiency of photocuring. The limited sensitivity of flash photolysis prevents its successful application in monitoring submicromolar concentrations of radicals typically employed in these reactions. Our own interest in developing a

(1) Davidson, R. S.; Dias, A. A.; Illsley, D. *J. Photochem. Photobiol. A: Chem.* **1995**, *89*, 75−87.
(2) Allen, N. S. *J. Photochem. Photobiol. A: Chem.* **1996**, *100*, 101−107.
(3) Porter, G.; Wilkinson, F. *Trans. Faraday Soc.* **1961**, *57*, 1686−1691.
(4) Bell, J. A.; Linschitz, H. *J. Am. Chem. Soc.* **1963**, *85*, 528−532.
(5) Godfrey, T. S.; Hilpern, J. W.; Porter, G. *Chem. Phys. Lett.* **1967**, *1*, 490−492.
(6) Tsubomura, H.; Yamamoto, N.; Tanaka, S. *Chem. Phys. Lett.* **1967**, *1*, 309−310.
(7) Buettner, A. V.; Dedinas, J. *J. Phys. Chem.* **1971**, *75*, 187−191.
(8) Ledger, M. B.; Porter, G. *J. Chem. Soc. Faraday Trans. 1* **1972**, *68*, 539−553.
(9) Porter, G.; Dogra, S. K.; Loutfy, R. O.; Sugamori, S. E.; Yip, R. W. *J. Chem. Soc., Faraday Trans. 1* **1973**, *69*, 1462−1474.
(10) Topp, M. R. *Chem. Phys. Lett.* **1975**, *32*, 144−149.
(11) Colman, P.; Dunne, A.; Quinn, M. F. *J. Chem. Soc., Faraday Trans. 1* **1976**, *72*, 2605−2609.
(12) Bensasson, R. V.; Gramain, J.-C. *J. Chem. Soc., Faraday Trans. 1* **1980**, *76*, 1801−1810.
(13) Encinas, M. V.; Scaiano, J. C. *J. Am. Chem. Soc.* **1981**, *103*, 6393−6397.
(14) Inbar, S.; Linschitz, H.; Cohen, S. G. *J. Am. Chem. Soc.* **1981**, *103*, 1048−1054.
(15) Nagarajan, V.; Fessenden, R. W. *Chem. Phys. Lett.* **1984**, *112*, 207−211.
(16) Baumann, H.; Merckel, C.; Timpe, H.-J.; Graness, A.; Kleinschmidt, J.; Gould, I. R.; Turro, N. J. *Chem. Phys. Lett.* **1984**, *103*, 497−502.
(17) Hiratsuka, H.; Yamazaki, T.; Maekawa, Y.; Hikida, T.; Mori, Y. *J. Phys. Chem.* **1986**, *90*, 774−778.
(18) Naguib, Y. M. A.; Steel, C.; Cohen, S. G. *J. Phys. Chem.* **1987**, *91*, 3033−3036.
(19) Johnston, L. J.; Hougnot, D. J.; Wintgens, V.; Scaiano, J. C. *J. Am. Chem. Soc.* **1988**, *110*, 518−524.
(20) Demeter, A.; László, B.; Bérces, T. *Ber. Bunsen-Ges. Phys. Chem.* **1988**, *92*, 1478−1485.

S0003-2700(97)01306-1 CCC: $15.00
Published on Web 05/19/1998

sensitive tool for monitoring triplet-ketone-derived radicals is to study H atom abstraction reactions at liquid/solid interfaces used for photobinding of molecules to polymer and other surfaces;[21,22] the limited number of surface sites at which reactions can occur in these systems imposes a sensitivity requirement in monitoring the transient radical population at the interface.

A potentially sensitive means of detecting aromatic radical intermediates produced in these photoreactions is to photoexcite the radical to its excited-doublet state[23] and monitor fluorescence from the excited radical. Fluorescence from the diphenylketyl radical or benzophenone ketyl radical has been studied in order to investigate the photophysics and photochemistry of the excited-doublet state.[15,20,23−37] The fluorescence decay time and quantum yield of the ketyl radical of benzophenone in toluene have been measured and were found to be $\tau_f = 3.9$ ns[32] and $\Phi_f = 0.11$,[38] respectively. The fluorescence decay time of the radical in more polar solvents is comparable (e.g., $\tau_f = 3.7$ ns in acetonitrile[28]), so the fluorescence quantum yield should also be significant in these solvents. While the fluorescence yield of the ketyl radical appears to be high enough for sensitive detection, the radical fluorescence emission is not resolved from phosphorescence of the precursor triplet state of benzophenone. If triplet-state phosphorescence can be independently measured and subtracted from the total emission signal, the time-resolved fluorescence transient of the ketyl radical can be isolated, and the kinetics of radical formation and recombination can be observed. In this work, time-resolved, continuous wave (cw) laser-excited fluorescence was resolved from other emission and scattering and used to detect nanomolar concentrations of diphenylketyl radicals derived from H atom abstraction by the triplet benzophenone. The ketyl radical populations were monitored on submicrosecond and millisecond time scales, and rate constants for radical formation and recombination were determined.

(21) Dunkirk, S. G.; Gregg, S. L.; Duran, L. W.; Monfils, J. D.; Haapala, J. E.; Marcy, J. A.; Clapper, D. L.; Amos, R. A.; Guire, P. E. *J. Biomater. Appl.* **1991**, *6*, 131−155.
(22) Ledwith, A. In *Photochemistry and Polymeric Systems*; Kelly, J. M., McArdle, C. B., de F.Maunder, M. J., Eds.; Royal Society of Chemistry: London, 1993; pp 1−14.
(23) Razi Naqvi, K.; Wild, U. P. *Chem. Phys. Lett.* **1976**, *41*, 570−574.
(24) Hodgson, B. W.; Keene, J. P.; Land, E. J.; Swallow, A. J. *J. Chem. Phys.* **1975**, *63*, 3671−3672.
(25) Mehnert, R.; Brede, O.; Helmstreit, W. *Z. Chem.* **1975**, *15*, 448−449.
(26) Topp, M. R. *Chem. Phys. Lett.* **1976**, *39*, 423−426.
(27) Obi, K.; Yamaguchi, H. *Chem. Phys. Lett.* **1978**, *54*, 448−450.
(28) Baumann, H.; Schumacher, K. P.; Timpe, H.-J.; Rehák, V. *Chem. Phys. Lett.* **1982**, *89*, 315−319.
(29) Thurnauer, M. C.; Meisel, D. *Chem. Phys. Lett.* **1982**, *92*, 343−348.
(30) Hiratsuka, H.; Yamazaki, T.; Takahashi, M.; Hikida, T.; Mori, Y. *Chem. Phys. Lett.* **1983**, *101*, 341−344.
(31) Baumann, H.; Merckel, C.; Timpe, H.-J.; Graness, A.; Kleinschmidt, J.; Gould, I. R.; Turro, N. J. *Chem. Phys. Lett.* **1984**, *103*, 497−502.
(32) Johnston, L. J.; Lougnot, D. J.; Scaiano, J. C. *Chem. Phys. Lett.* **1986**, *129*, 205−210.
(33) Hiratsuka, H.; Rajadurai, S.; Das, P. K.; Hug, G. L.; Fessenden, R. W. *Chem. Phys. Lett.* **1987**, *137*, 255−260.
(34) Johnston, L. J.; Lougnot, D. J.; Wintgens, V.; Scaiano, J. C. *J. Am. Chem. Soc.* **1988**, *110*, 518−524.
(35) Yankov, P.; Nickolov, Zh.; Zhelyaskov, V.; Petkov, V. *J. Photochem. Photobiol. A: Chem.* **1989**, *47*, 155−165.
(36) Redmond, R. W.; Scaiano, J. C.; Johnston, L. J. *J. Am. Chem. Soc.* **1992**, *114*, 9768−9773.
(37) Figuera, J. M.; Sastre, R.; Costela, A.; Garcia-Moreno, I.; Al-Hakakk, M. T.; Dabrio, J. *Laser Chem.* **1994**, *15*, 33−46.

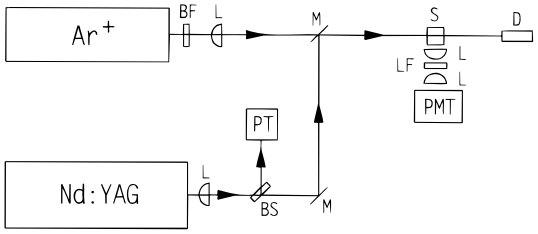

Figure 1. Laser-induced time-resolved fluorescence experiment. L is a lens, BS is a beam splitter, M is a mirror, BF is a 514.5-nm band-pass filter, LF is a liquid filter to block 355-nm irradiation, S is the sample, D is a beam dump. PT is a vacuum phototube used to trigger the scope, and PMT is a photomultiplier tube used to detect emission from the sample.

EXPERIMENTAL SECTION

Instrumentation. The experimental setup is shown in Figure 1. A Quanta Ray model GCR-11 Q-switched Nd:YAG laser was operated at 10 Hz and blocked by a shutter to provide a repetition rate of 0.1−1.0 Hz; the beam was frequency tripled ($\lambda_e = 355$ nm), and the 5-ns UV (100−600 μJ) pulse was weakly focused to a spot size of 2.2 mm and used to photoexcite the sample. Fluorescence of transient diphenylketyl radicals was excited by a beam from a Lexel model 95 cw argon ion laser ($\lambda_p = 514.5$ nm), which was focused to a spot size of 380 μm in the sample with power varied between 50 and 500 mW.

Fluorescence and phosphorescence were collected at 90° from the excitation axis and filtered through a 1.0-cm path of a ≈5% aqueous solution of sodium nitrite and three glass filters (Schott KV408, KV550, and OG570). The filtered emission was detected by a Hamamatsu R976 photomultiplier tube, digitized with a LeCroy 9450 oscilloscope with the input termination at 1 kΩ, and averaged.

For microsecond radical formation kinetics, the Nd:YAG laser photolysis pulse energy was 150 μJ, and the cw probe laser power was 500 mW; the signal voltage was derived from a 1-kΩ termination resistor, giving an RC time constant of 0.1 μs. The sample solution was stirred to provide a fresh sample in the excitation region, and 100 transients were averaged for each data record. For studies of radical recombination kinetics on a 100-ms time scale, the effect of stirring could be observed as structure in the residuals. For these slower experiments, therefore, stirring was not used, and a lower repetition rate, 0.1 Hz, was chosen to allow diffusion to replace the reacted population in the beam between experiments. The signal voltage was derived from a larger termination resistance of 1 MΩ, which yields an RC time constant of 100 μs. Ten transients were averaged for each data record; the excitation laser energy was varied between ≈100 and 600 μJ/pulse to vary the radical concentration, and the cw probe laser power was tested at two levels, 50 and 500 mW, to determine the influence of radical photobleaching on the results.

Reagents and Solutions. Benzophenone (Aldrich, +99%), benzhydrol (Aldrich, 99%), acetonitrile (OmniSolv, glass distilled), and 2-propanol (OmniSolv, glass distilled) were used without further purification. Oxygen was removed from the benzophenone solutions by four freeze−pump−thaw cycles, pumped to a base pressure of ≤50 μTorr. Under these conditions, a 100 μM solution of benzophenone produced an unquenched triplet lifetime of ≈200 μs. The concentration of benzophenone was 100 μM, and solutions were kept at room temperature unless otherwise

specified. To reduce the effect of sample photolysis on the results, 10 mL of solution was placed in the 1-cm path length quartz freeze−pump−thaw cell, and the sample was shaken several times after each set of 10 transients was collected.

Data Analysis. Phosphorescence transients from triplet benzophenone were fit to a first-order decay model to determine the ketyl radical formation (H atom abstraction) rate constant. When detecting fluorescence from the diphenylketyl radical, phosphorescence emission from the pulsed-laser-excited triplet state of benzophenone appears as a background interference, since the fluorescence maximum of the excited radical is ≈565 nm,[24] while phosphorescence emission from benzophenone triplet extends beyond 600 nm.[36] Fluorescence from the excited diphenylketyl radical was isolated by subtracting the phosphorescence emission (355-nm pulsed excitation only) measured independently. Scattering from the cw argon ion laser (514.5-nm illumination only) and the radio frequency (rf) interference from the Q-switch were also subtracted.

Time-resolved fluorescence transients were fit to their respective kinetic models, compiled in Microsoft Fortran using a Marquardt algorithm to optimize the kinetic parameters and intensities. Each fluorescence measurement was done in triplicate, so kinetic parameters and uncertainties could be estimated from a weighted linear least-squares analysis and Student's *t*-statistics. The uncertainties in rate constants are reported at the 95% confidence level, while error bars are plotted to indicate ±1 standard deviation.

RESULTS AND DISCUSSION

The use of laser-excited fluorescence to monitor the formation and decay of a photogenerated radical population was tested for ketyl radicals derived from the H atom abstraction by the excited-triplet state of benzophenone from 2-propanol. Below is shown the reaction scheme for the photoreduction of triplet benzophenone by alcohols,[39−46] using 2-propanol as the specific example.

$$Ph_2CO + h\nu \rightarrow {}^1Ph_2CO \rightarrow {}^3Ph_2CO \quad (1a)$$

$${}^3Ph_2CO \xrightarrow{k_0} Ph_2CO \quad (1b)$$

$${}^3Ph_2CO + (CH_3)_2CHOH \xrightarrow{k_H} Ph_2\dot{C}OH + (CH_3)_2\dot{C}OH \quad (2)$$

$$2(CH_3)_2\dot{C}OH \xrightarrow{k_2} ((CH_3)_2COH)_2,\ (CH_3)_2CHOH + (CH_3)_2CO \quad (3)$$

$$(CH_3)_2\dot{C}OH + Ph_2\dot{C}OH \rightarrow \text{mixed pinacol},\ (CH_3)_2CHOH + Ph_2CO,\ (CH_3)_2CO + Ph_2CHOH \quad (4)$$

$$(CH_3)_2\dot{C}OH + Ph_2CO \xrightarrow{k_{at}} (CH_3)_2CO + Ph_2\dot{C}OH \quad (5)$$

$$2\ Ph_2\dot{C}OH \xrightarrow{k_r} (Ph_2COH)_2 \quad (6)$$

The triplet state of benzophenone is produced in step 1a via photoexcitation to the excited-singlet state and subsequent intersystem crossing to the triplet manifold. Phosphorescence and nonradiative decay of the triplet state to the ground state occur in step 1b. The triplet state also decays via reactive quenching by 2-propanol,[3,43] producing the diphenylketyl radical and the isopropylol radical by hydrogen atom abstraction from the alcohol in step 2. Decay of the isopropylol radical occurs through recombination with another quencher radical (step 3), recombination with a diphenylketyl radical (step 4), and an atom-transfer reaction with ground-state benzophenone (step 5), which also produces a diphenylketyl radical. The ketyl radical decays predominantly by a second-order combination reaction (step 6).[41,47]

Ketyl Radical Formation Kinetics. The H atom abstraction kinetics to produce the ketyl radical from the excited-triplet state of benzophenone were first determined from the quenching of benzophenone phosphorescence. These data were collected and fit to a first-order model for the decay of the triplet population: $I_p(t) = A_p \exp(-k_{obs}t)$, where A_p is the initial phosphorescence intensity and $k_{obs} = (k_0 + k_H[(CH_3)_2CHOH])$, where k_0 is the unquenched rate of phosphorescence decay and k_H is the rate constant for quenching by H atom abstraction. The 2-propanol concentration was varied to determine the influence of the quencher on the decay of the triplet population. Figure 2a shows example phosphorescence transients together with the best fit to a first-order decay model for 2-propanol concentrations ranging from 50 to 200 mM. The measured decay rates are plotted versus the 2-propanol concentrations in a Stern−Volmer analysis, as shown in Figure 3a; the quenching rate constant was determined from the slope to be $k_H = (2.1 \pm 0.1) \times 10^6\ M^{-1}\ s^{-1}$. These phosphorescence decay results provide an independent measurement of k_H to compare with data from ketyl radical fluorescence.

Fluorescence from the initially formed diphenylketyl radical population was excited with a 500-mW, cw 514.5-nm beam from an argon ion laser. Benzophenone phosphorescence background is also present in the luminescence signal. This background was measured independently, with the argon ion laser beam blocked, and subtracted from the total luminescence signal. In addition, the 514.5-nm scattering and rf background were measured, with the 355-nm photolysis laser operating but with the beam blocked, and the result was subtracted from the total luminescence signal. Figure 4a shows the total luminescence, phosphorescence, and the rf and scattering background signals with the resulting ketyl radical fluorescence transient (Figure 4b) following background subtraction. The formation kinetics of the radical population were monitored for 2-propanol concentrations ranging from 50 to 750 mM, and the results are plotted in Figure 3b. Diphenylketyl radicals are formed by photoreduction of the benzophenone triplet

(38) Redmond, R. W.; Scaiano, J. C. *Chem. Phys. Lett.* **1990**, *166*, 20−25.
(39) Bäckström, H. L. J. In *The Svedberg, 1884−1944, 60th Birthday Memorial Volume*; Almqvist and Wiksells Boktryckeri: Stockholm, Sweden, 1944; pp 45−64.
(40) Schenck, G. O.; Mader, W.; Pape, M. *Proc. Int. Conf. Peaceful Uses At. Energy.* **1958**, *29*, 352−363.
(41) Pitts, Jr., J. N.; Letsinger, R. L.; Taylor, R. P.; Patterson, J. M.; Recktenwald, G.; Martin, R. B. *J. Am. Chem. Soc.* **1959**, *81*, 1068−1077.
(42) Moore, W. M.; Hammond, G. S.; Foss, R. P. *J. Am. Chem. Soc.* **1961**, *83*, 2789−2794.
(43) Beckett, A.; Porter, G. *Trans. Faraday Soc.* **1963**, *59*, 2038−2050.
(44) Bäckström, H. L. J.; Appelgren, K. L.; Niklasson, R. J. V. *Acta Chem. Scand.* **1965**, *19*, 1555−1565.
(45) Filipescu, N.; Minn, F. L. *J. Am. Chem. Soc.* **1968**, *90*, 1544−1547.
(46) Weiner, S. A. *J. Am. Chem. Soc.* **1971**, *93*, 425−429.
(47) Schuster, D. I.; Karp, P. B. *J. Photochem.* **1980**, *12*, 333−344.

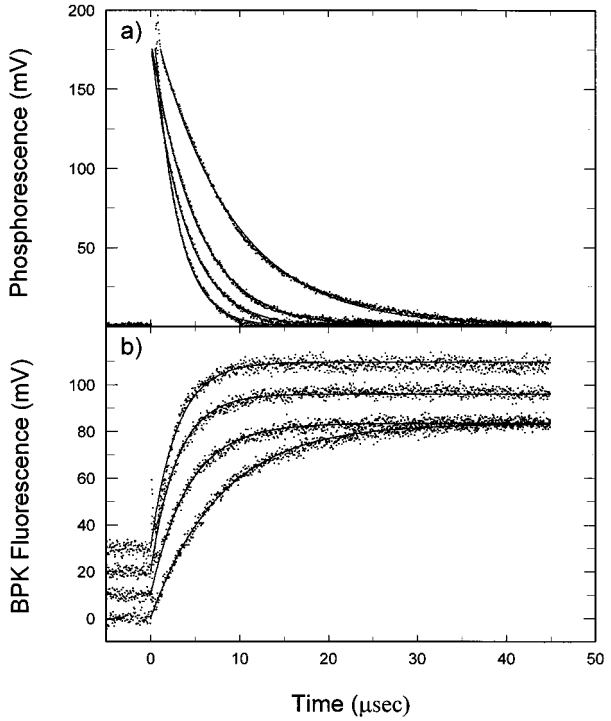

Figure 2. Luminescence signals from the reaction of benzophenone with 2-propanol. (a) Phosphorescence emission from triplet benzophenone in acetonitrile quenched by 2-propanol at 50, 100, 150, and 200 mM. The smooth curves are the best fits to a first-order decay model. (b) Continuously excited fluorescence transients from diphenylketyl radicals produced by the reaction of triplet benzophenone with 2-propanol at 50, 100, 150, and 200 mM; the smooth curves are the best fits to a first-order formation model. Note: the transients taken with higher concentrations of 2-propanol are each offset by 10 mV for viewing.

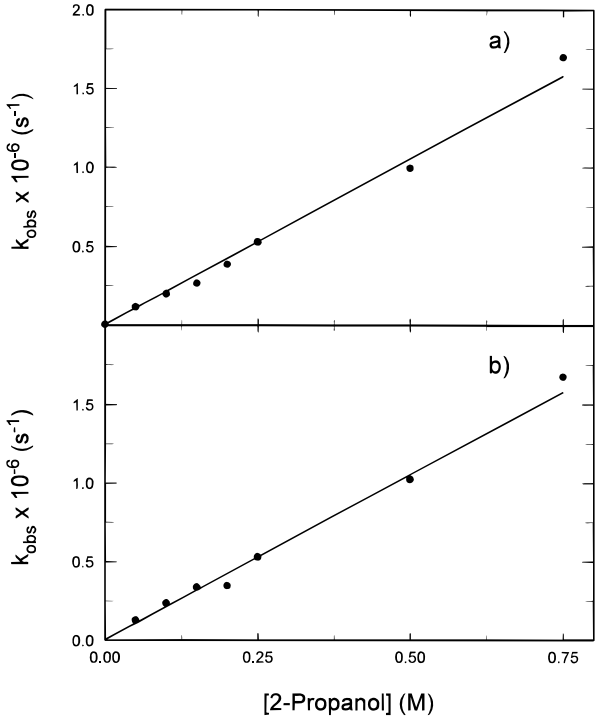

Figure 3. (a) Stern−Volmer plot of the benzophenone phosphorescence decay rate, k_{obs}, versus 2-propanol concentration. The H atom abstraction rate constant from the slope of the plot (with the intercept fixed at the measured unquenched decay rate of the phosphorescence, $k_0 = 5100\ s^{-1}$) is determined to be $(2.1 \pm 0.1) \times 10^6\ M^{-1}\ s^{-1}$. (b) Stern−Volmer plot of the ketyl radical fluorescence appearance rate, k_{obs}, versus 2-propanol concentration. The H atom abstraction rate constant from the slope (with the intercept fixed as above) is $(2.1 \pm 0.1) \times 10^6\ M^{-1}\ s^{-1}$.

state via H atom abstraction by 2-propanol, as shown in step 2 of the reaction scheme. If this is the only step producing ketyl radicals, then solving the differential equation for the radical formation leads to a simple first-order growth model for the fluorescence intensity versus time: $I_f(t) = A_f[1 - \exp(-k_{obs}t)]$. The fluorescence data are fit to this model, and the results are plotted with the data in Figure 2b.

While the decay of the triplet population of benzophenone is expected to be a simple first-order process (since, at these low excited-state concentrations, triplet−triplet annihilation can be neglected[48,49]), the formation kinetics of the ketyl radical can be more complicated, since an additional reaction (step 5, above) can also produce radicals. This step involves an H atom-transfer reaction between the isopropylol radical, $(CH_3)_2\dot{C}OH$, and ground-state benzophenone. Due to the modest reaction rate constant for H atom transfer ($\approx 1 \times 10^5\ M^{-1}\ s^{-1}$ [20,50,51]) and the low concentration of benzophenone (100 μM), the production of ketyl radicals from the atom-transfer step occurs on a millisecond time scale, much slower than the rate of initial radical production by the H atom abstraction from the alcohol. Therefore, the fluorescence data collected on the microsecond time scale fit a first-order growth model, as can be seen in Figure 2b and in the lack of structure in the residuals. The measured first-order rates determined from these fits were plotted versus 2-propanol concentration in Figure 3b to determine the radical formation rate constant. The result, $k_H = (2.1 \pm 0.1) \times 10^6\ M^{-1}\ s^{-1}$, was identical to the value determined from phosphorescence decay data. The rate constant is also indistinguishable from that reported in a flash photolysis (transient absorption) study by Demeter and Bérces,[52] where $k_H = (2.3 \pm 0.3) \times 10^6\ M^{-1}\ s^{-1}$.

Estimating the Concentration of Ketyl Radicals. To assess the fluorescence detection limits for ketyl radicals, their initial concentration in the probe laser beam was estimated as follows. Since the probe beam spot size ($w_p = 380\ \mu m$) is much smaller than that of the pulsed excitation laser beam ($w_e = 2.2$ mm), the concentration of radicals in the probe beam is governed by the fluence of the excitation laser at its center: $\rho_{h\nu} = 2E_p/[(h\nu)\pi w_e^2]$, where E_p is the pulse energy of the excitation beam (J), $h\nu$ is the excitation laser photon energy at 355 nm (J/photon), and w_e is the excitation spot size (cm). Under weak photolysis conditions, the fluence (in photons/cm^2) times the absorption cross section, σ_a (in cm^2), of benzophenone at 355 nm determines the fraction of benzophenone ground states that are photoexcited; the fraction of excited states that react with 2-propanol to form ketyl radicals is $\phi_k = k_H[(CH_3)_2CHOH]/(k_0 + k_H[(CH_3)_2CHOH])$, which results

(48) Kellogg, R. E. *J. Chem. Phys.* **1964**, *41*, 3046−3047.
(49) Yekta, A.; Turro, N. J. *Mol. Photochem.* **1972**, *3*, 307−322.
(50) Demeter, A.; Bérces, T. *J. Phys. Chem.* **1991**, *95*, 1228−1232.
(51) Viltres Costa, C.; Grela, M. A.; Churio, M. S. *J. Photochem. Photobiol. A: Chem.* **1996**, *99*, 51−56.
(52) Demeter, A.; Bérces, T. *J. Photochem. Photobiol. A: Chem.* **1989**, *46*, 27−40.

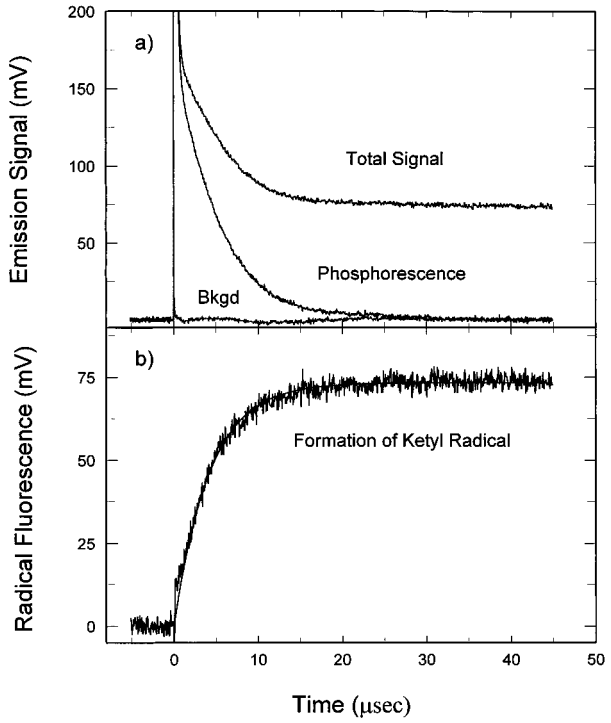

Figure 4. Isolating the diphenyketyl radical fluorescence signal. (a) Total luminescence signal (355-nm pulsed Nd:YAG and cw 514.5-nm laser excitation), phosphorescence (355-nm pulsed Nd:YAG only), and the rf and scattering background signals (cw 514.5-nm laser only). (b) Subtracting the phosphorescence and the rf and scattering background results in the isolated BPK fluorescence signal.

in an expression for the initial concentration of diphenylketyl radicals immediately following the decay of the triplet benzophenone population:

$$[\mathrm{Ph_2\dot{C}OH}] = \sigma_a \rho_{h\nu} \phi_k [\mathrm{Ph_2CO}] \qquad (7)$$

This expression is used to estimate the radical concentration for the data presented in Figure 4. Based on the measured H atom abstraction rate constant, k_H, the quantum yield of radical formation is nearly unity for this experiment, $\phi_k = 97.8\%$; the modest excitation laser pulse energy (150 μJ) and large spot size (2.2 mm), however, result in a small fraction (0.13%) of the 100 μM ground-state benzophenone concentration being excited. The concentration of ketyl radicals producing the signal plateau in Figure 4 is $[\mathrm{Ph_2\dot{C}OH}] = 130$ nM. Based on the observed signal-to-noise ratio of this transient, the quantitation limit (10σ) for radical fluorescence detected on a microsecond time scale is ≈45 nM, which is quite adequate for monitoring the formation of small radical populations used to initiate chain reaction processes.

Fluorescence Monitoring of Radical Decay Kinetics. In the absence of other reactive substrates or radical scavengers in the system, the diphenylketyl radical population is expected to decay by radical recombination (steps 4 and 6 in the reaction scheme). Since these reactions are second-order processes, the concentration of radicals affects the rate of recombination and can be used as a variable to determine the reaction rate constant. A simple method to vary the concentration of radicals in the beam, without influencing other reaction rates in the system, is to regulate the fluence of the excitation laser, which controls the concentration of excited states that are initially generated in the beam, as shown in eq 7 above.

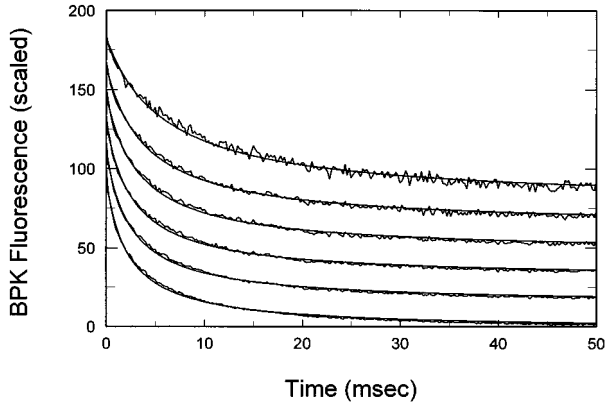

Figure 5. Monitoring BP ketyl radical decay kinetics. Benzophenone (100 μM in ACN) is reacted with 250 mM 2-propanol to generate radicals. Fluorescence from the BP ketyl radical population is continuously excited with 500 mW at 514.5 nm. The 355-nm excitation laser pulse energy is varied from top to bottom as follows: 90, 190, 260, 380, 470, and 590 μJ. The transients are scaled to the same amplitude, offset for viewing, and fit to a second-order decay model, eq 9.

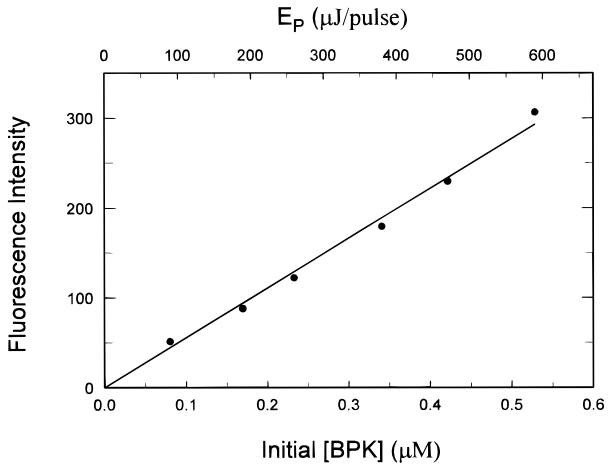

Figure 6. Initial BP ketyl fluorescence amplitude versus excitation pulse energy. The initial diphenylketyl radical concentration predicted by eq 7 is also plotted as the lower *x*-axis. See conditions in the caption of Figure 5.

An example set of data where radical recombination is monitored by laser-excited fluorescence is shown in Figure 5, where the excitation laser pulse energy is varied between 90 and 590 μJ/pulse, which generates initial radical concentrations ranging from 80 to 530 nM at the center of the beam based on eq 7. For low concentrations of these species (where self-absorption and self-quenching can be neglected), the amplitude of the fluorescence signal should be proportional to the photogenerated radical concentration. A plot of the initial fluorescence intensity versus excitation laser energy (and the corresponding radical concentration) is shown in Figure 6; the plot is linear, and the intercept is zero within its uncertainty. These results indicate that the radical concentration can be controlled by the excitation laser pulse energy. The variation of pulse energy does not significantly change the excitation beam spot size or alignment; otherwise, the radical population would not have varied linearly with E_p.

The effect of the change in radical concentration on the rate of radical recombination is apparent in the fluorescence transients plotted in Figure 5. The greater radical concentration generated at higher excitation laser energies decays at a faster rate, as expected from a second-order reaction model. The rates of recombination and disproportionation between isopropylol radicals (k_2, step 3) are much faster than rates of reactions between the isopropylol and diphenylketyl radicals (step 4), as determined by studies of reaction products where no mixed pinacol or benzhydrol was detected.[41] As a result, decay of the diphenylketyl radical population should be dominated by homolytic recombination (step 6), the rate of which is given by

$$\frac{\mathrm{d}[\mathrm{Ph_2\dot{C}OH}]}{\mathrm{d}t} = -2k_r[\mathrm{Ph_2\dot{C}OH}]^2 \qquad (8)$$

Separation of variables and integration over time yields a second-order kinetic expression:

$$[\mathrm{Ph_2\dot{C}OH}]_t = \frac{[\mathrm{Ph_2\dot{C}OH}]_{t=0}}{1 + \alpha t} \qquad (9)$$

where α is the initial decay rate of radicals relative to their initial concentration,

$$\alpha = 2k_r[\mathrm{Ph_2\dot{C}OH}]_{t=0} \qquad (10)$$

The fluorescence transients in Figure 5 were fit to this decay model, and the residual error is comparable to the noise in the data, as shown in the figure.

While the radical decay results are consistent with kinetics dominated by homolytic recombination, the concentration of diphenylketyl radicals in the reaction is uncertain due to atom transfer between an isopropylol radical, $(CH_3)_2\dot{C}OH$, and ground-state benzophenone (step 5 in the reaction scheme). As discussed above, this reaction can be neglected as a significant source of radicals on a microsecond time scale; however, with high concentrations of benzophenone (BP) in the sample, this reaction can increase the radical concentration on the longer (millisecond) time scale, in which recombination is observed. The higher benzophenone ketyl (BPK) radical concentration would generate a faster second-order decay rate than expected for the radical concentration predicted by eq 7 and produce an error in the reported rate constant for ketyl radical recombination. If this step has a significant yield under these conditions, then the data should follow a model that includes this growth step in addition to the second-order decay; there may be some evidence of this process in the slightly higher fluorescence intensities observed in the data in Figure 5 in the 5−10-ms time region. Fitting the data in Figure 5 to a model that includes atom-transfer formation of BPK radicals, however, does not lead to a statistically significant improvement in the fit compared to a simple second-order decay model. Therefore, formation kinetics of diphenylketyl radical by atom transfer (step 5) could not be determined directly from these data. The influence of the atom transfer kinetics can, however, be detected in these results when they are compared to recombination of diphenylketyl radicals derived in the absence of the atom-transfer process.

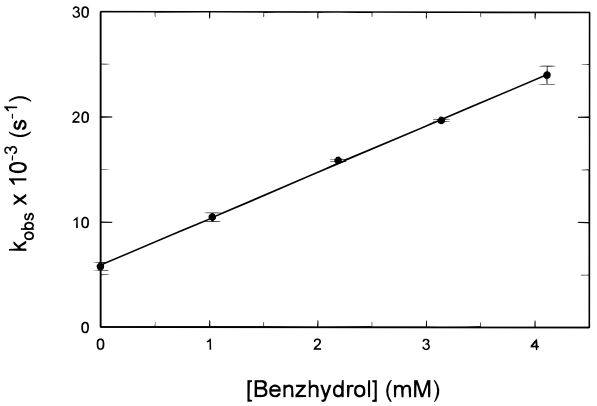

Figure 7. Stern−Volmer plot of the benzophenone phosphorescence decay rate, k_{obs}, versus benzhydrol concentration. The H atom abstraction rate constant from the slope of the plot is $k_H = (4.4 \pm 0.1) \times 10^6\ M^{-1}\ s^{-1}$.

Measurement of the Diphenylketyl Radical Recombination Rate Constant. To measure the rate of recombination of diphenylketyl radicals in the absence of step 5, the BPK radicals can be formed by reaction of the triplet state of benzophenone with benzhydrol (BPH_2):

$$^3\mathrm{Ph_2CO} + \mathrm{Ph_2CHOH} \rightarrow 2\mathrm{Ph_2\dot{C}OH} \qquad (11)$$

In this simple reaction, two diphenylketyl radicals are derived from the H atom abstraction step with the following quantum yield for formation:

$$\phi_k = \frac{2k_H[\mathrm{BPH_2}]}{k_0 + k_H[\mathrm{BPH_2}]} \qquad (12)$$

Thus, there are no additional radical species derived from the quencher to undergo an atom transfer with ground-state BP (no step 5). In addition, the only decay route for the ketyl radical is through recombination with another ketyl radical.

To study the BP/BPH_2/ACN system, the quenching rate constant had to be determined so that the radical yield was known. The benzhydrol concentration was varied from 0 to 4 mM, and phosphorescence decay data were collected as above and fit to a pseudo-first-order decay model. A Stern−Volmer plot of the observed rate versus benzhydrol concentration (Figure 7) results in an H atom abstraction rate constant of $(4.4 \pm 0.2) \times 10^6\ M^{-1}\ s^{-1}$. This rate constant falls within the range from 4×10^6 to $(5.2 \pm 0.3) \times 10^6\ M^{-1}\ s^{-1}$ previously reported in the literature.[12,52]

The measured rate constant for H atom abstraction was used together with the unquenched lifetime of triplet benzophenone ($1/k_o = 180\ \mu s$) in eq 12 to predict the quantum yield of diphenylketyl radical formation. The radical recombination kinetics were measured by using a 1 mM concentration of benzhydrol to quench the triplet excited state ($\phi_k = 0.86$) and by varying the excitation laser pulse energy as in Figures 5 and 6 to control the concentration of radicals. Transients of the form shown in Figure 5 were fit to the second-order decay model of eq 9, and the second-

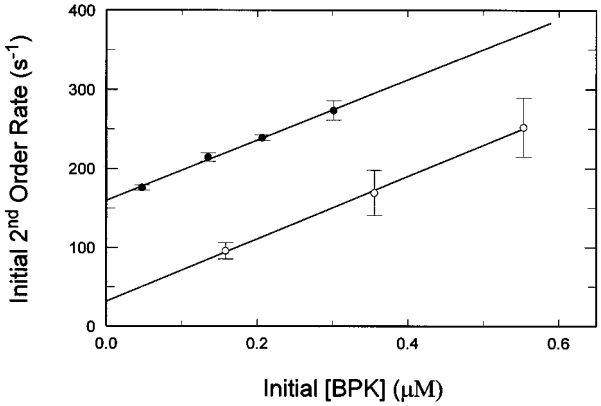

Figure 8. Second-order initial ketyl radical recombination rate versus the initial ketyl radical concentration. Diphenylketyl radicals were derived from quenching of triplet benzophenone by benzhydrol in acetonitrile, and their concentration was varied by changing the excitation pulse energy. Solid points are rates measured using 500-mW cw probe power and 100 μM benzophenone, $k_r = (1.9 \pm 0.2) \times 10^8$ M^{-1} s^{-1}; open circles are rates measured using 50-mW probe power and 250 μM benzophenone, $k_r = (2.0 \pm 0.6) \times 10^8$ M^{-1} s^{-1}.

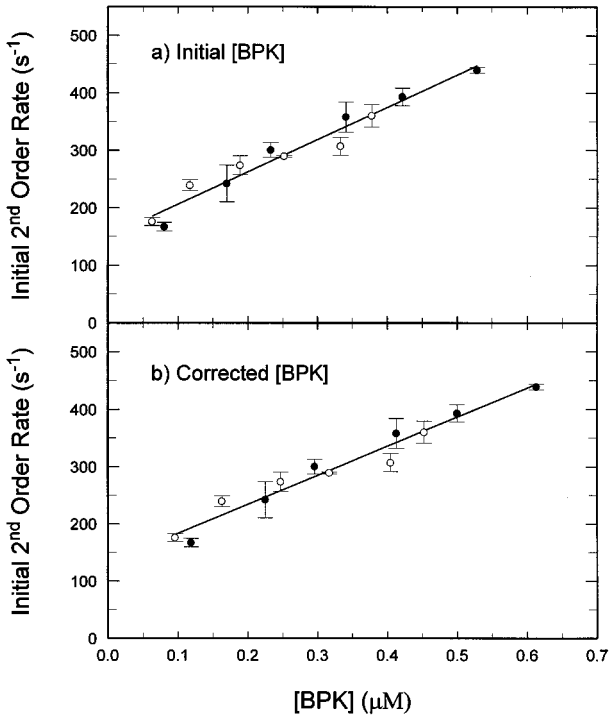

Figure 9. Second-order initial radical recombination rate versus ketyl radical concentration. Diphenylketyl radicals are derived from quenching of triplet benzophenone by 2-propanol at two concentrations: filled points are from 250 mM, open points are from 750 mM. The radical concentrations were varied by changing the excitation fluence, and the probe power was 500 mW. (a) *x*-Axis based on the initial concentration of radicals formed immediately after the laser pulse; the apparent radical recombination rate constant from the slope is $k_{r,app} = (2.8 \pm 0.4) \times 10^8$ M^{-1} s^{-1}. (b) *x*-Axis based on the concentration of radicals corrected for the atom-transfer yield estimated by eq 13, where the resulting recombination rate constant is $k_r = (2.5 \pm 0.4) \times 10^8$ M^{-1} s^{-1}.

order initial rates, α, are plotted against the initial concentration of radicals in Figure 8 for two different probe powers, 50 and 500 mW. The slope of these plots can be used to determine the diphenylketyl radical recombination rate constant, as in eq 10. The resulting rate constants are $k_r = (2.0 \pm 0.6) \times 10^8$ M^{-1} s^{-1} for probing with a 50-mW beam and $k_r = (1.9 \pm 0.2) \times 10^8$ M^{-1} s^{-1} for 500-mW probe power, which agree within their error range. These results are similar in magnitude to the rate constant for diphenylketyl radical recombination in acetonitrile reported by Naquib et al.,[53] $k_r = 1.0 \times 10^8$ M^{-1} s^{-1}.

The two probe powers were tested in order to explore the nonzero intercept observed at higher powers. As shown in eq 10, the rate of second-order recombination should vanish at zero radical concentration, but the plot at higher probe power shows a significant intercept. This indicates that an additional kinetic process, which does not depend on radical concentration, is contributing to the decay of the population. Since the intercept rate vanishes at the 10-fold lower probe power, the results appear to indicate that photobleaching of diphenylketyl radicals significantly influences their decay kinetics when monitored at higher probe powers. Photobleaching of diphenylketyl radicals has previously been reported.[15,34,36] Nagarajan and Fessenden reported photobleaching of BPK radicals and attributed the reaction to the excited radical acting as an H atom donor.[15] Johnston et al.[34] reported photobleaching of diphenylketyl radicals at a high yield at 515 nm ($\phi_{bl} = 0.27$) and suggested that its origin was O−H bond cleavage to give benzophenone and an H atom. The rate of radical disappearance in the intercept of Figure 8 (top) can be used to estimate the photobleaching yield of diphenylketyl radicals in the 500-mW probe power experiment; from the average probe beam intensity and the estimated molar absorptivity of the radical at 514.5 nm (2.5×10^3 M^{-1} cm^{-1} [24]), the rate of radical loss at the origin (160 s^{-1}), which is independent of radical concentration, is consistent with a photobleaching yield of $\phi_{bl} = 0.06 \pm 0.01$. This value is 4.5 times smaller than that reported by Johnston et al.;[34] in their work, however, a 100-mJ pulsed laser was used to probe the radical fluorescence, having a peak power nearly 6 orders of magnitude greater than that of the cw probe laser used in this work. It is possible that their higher photobleaching yield could arise from up-pumping of the excited-doublet state of the radical.

Detecting Diphenylketyl Radicals Produced by Atom Transfer. In the study of benzophenone quenched by 2-propanol in acetonitrile discussed above, the diphenylketyl radical concentration can be increased over the initial population formed during the quenching of triplet benzophenone by H atom transfer from the isopropylol radical and ground-state benzophenone (step 5 in the reaction scheme). The influence of this population can be detected in the rate of recombination of the BPK radicals derived from 2-propanol quenching, as shown in Figure 9. Note that the probe power was 500 mW for this study to improve the S/N ratio in the data; the intercept rate was identical to that observed in the benzhydrol quenching study discussed above. Neglecting any contribution to the diphenylketyl radical concentration from the H atom-transfer step, the second-order initial recombination rate was plotted versus the initial ketyl radical concentration and used to calculate an apparent recombination rate constant, $k_{r,app} = (2.8 \pm 0.4) \times 10^8$ M^{-1} s^{-1} (see Figure 9a). This rate constant is significantly higher than the actual recombination rate constant

(53) Naguib, Y. M. A.; Cohen, S. G.; Steel, C. *J. Am. Chem. Soc.* **1986**, *108*, 128−133.

derived from the benzhydrol quenching study above. The additional diphenylketyl radical population that can arise from H atom transfer (step 5) on a millisecond time scale could account for the 40% higher apparent rate constant for recombination.

To determine the impact that atom transfer would be expected to have on the diphenylketyl radical concentration under these conditions, the steady-state atom-transfer yield, Φ_{at}, was estimated for each isopropylol concentration using the following equation:[54]

$$\phi_{at} = \frac{\ln (1 + \beta/2)}{\beta/2} \tag{13}$$

where $\beta = \alpha_2/k_1$ is the ratio of the second-order initial rate of isopropylol radical recombination and disproportionation, $\alpha_2 = 2k_2[(CH_3)_2\dot{C}OH]_{t=0}$, to the pseudo-first-order rate constant for atom transfer, $k_1 = k_{at}[Ph_2CO]$. As shown in step 2 of the reaction scheme, the initial concentration of the isopropylol radical was assumed to be equal to the initial diphenylketyl radical concentration, calculated from the excitation laser fluence using eq 7. Literature values for the combined rate constant for isopropylol radical recombination and disproportionation, $k_2 = 1.3 \times 10^9$ M^{-1} s^{-1},[20] and the atom-transfer reaction rate constant, $k_{at} = 3.6 \times 10^5$ M^{-1} s^{-1},[50] were used in eq 13 to estimate the steady-state atom-transfer yields (at the benzophenone concentration of 100 μM).

The estimated yields range from 52% at low fluence to 16% at high fluence conditions; the atom transfer yields drop at higher radical concentrations as the rate of the second-order recombination (step 3) increases, which competes with the pseudo-first-order rate of atom transfer. These yields were used to adjust the diphenylketyl radical concentrations for the additional population arising from atom transfer (step 5), and the measured radical recombination rates were replotted versus the corrected BPK concentrations in Figure 9b. The recombination rate constant derived from the slope of this plot is $k_r = (2.5 \pm 0.4) \times 10^8$ M^{-1} s^{-1}, smaller than the value based on the initial BPK population. This recombination rate constant agrees at the limit of its uncertainty with the value determined from the benzhydrol quenching experiment, indicating that atom transfer between isopropylol radicals and benzophenone contributes to the diphenylketyl radical concentration and influences the measured rate of radical recombination.

(54) Cambron, R. T.; Harris, J. M. *J. Phys. Chem.* **1994**, *98*, 8726−8733.

Finally, correcting the radical population for the contribution from H atom transfer allows the quantitation limit for fluorescence monitoring of diphenylketyl radicals to be assessed on the longer, 100-ms time scale of radical recombination. From the amplitude of the residuals in the lowest concentration BPK fluorescence transient of Figure 5, the quantitation limit (10σ) for radical fluorescence detected on a millisecond time scale is 20 nM, which is adequate for monitoring the decay of dilute populations typically used in initiating radical chain processes.

Conclusion. Monitoring of the photolytic initiation of free radical reactions requires time-resolved detection of submicromolar concentrations of radicals to provide information about rates of initiation and their competition with radical recombination. In this work, cw-laser excited fluorescence emission was shown to be a viable approach for monitoring aromatic radicals that are produced in type II photoinitiation of these reactions. Specifically, diphenylketyl radicals produced by photoreduction of the triplet state of benzophenone were readily detected at nanomolar concentrations, and their formation and decay kinetics were monitored in solution on time scales from a few microseconds to hundreds of milliseconds. H atom abstraction by triplet benzophenone from both 2-propanol and benzhydrol were measured, and the rate constants were found to be $k_H = (2.1 \pm 0.1) \times 10^6$ M^{-1} s^{-1} for 2-propanol and $k_H = (4.4 \pm 0.1) \times 10^6$ M^{-1} s^{-1} for benzhydrol. The diphenylketyl radical recombination rate constant was also determined by time-resolved fluorescence monitoring of the decay of the radical population and found to be $k_r = (1.9 \pm 0.2) \times 10^8$ M^{-1} s^{-1}. Photobleaching of radicals was shown to affect the population decay kinetics when probe laser intensity is large. Varying the probe intensity provides a test for this process, which does not influence the value of the rate constant for radical recombination when determined by varying the radical concentration. Formation kinetics could be measured on a microsecond time scale from radical populations as low as 45 nM; decay kinetics could be followed on a millisecond time scale from 20 nM concentrations.

ACKNOWLEDGMENT

This research was supported in part by the National Science Foundation under Grant CHE95-10312.

Received for review December 3, 1997. Accepted March 25, 1998.

AC9713060